



Inhibition of secreted phospholipases A₂ by 2-oxoamides based on α -amino acids: Synthesis, in vitro evaluation and molecular docking calculations

Varnavas D. Mouchlis^a, Victoria Magrioti^a, Efrosini Barbayianni^a, Nathan Cermak^b, Rob C. Oslund^b, Thomas M. Mavromoustakos^a, Michael H. Gelb^b, George Kokotos^{a,*}

^aLaboratory of Organic Chemistry, Department of Chemistry, University of Athens, Panepistimiopolis, Athens 15771, Greece

^bDepartment of Chemistry and Biochemistry, University of Washington, Seattle, WA 98195, USA

ARTICLE INFO

Article history:

Received 20 September 2010

Revised 7 December 2010

Accepted 13 December 2010

Available online 16 December 2010

Keywords:

GOLD

Molecular docking

2-Oxoamides

Phospholipase A₂

Simulated annealing

ABSTRACT

Group IIA secreted phospholipase A₂ (GIIA sPLA₂) is a member of the mammalian sPLA₂ enzyme family and is associated with various inflammatory conditions. In this study, the synthesis of 2-oxoamides based on α -amino acids and the in vitro evaluation against three secreted sPLA₂s (GIIA, GV and GX) are described. The long chain 2-oxoamide GK126 based on the amino acid (S)-leucine displayed inhibition of human and mouse GIIA sPLA₂s (IC₅₀ 300 nM and 180 nM, respectively). It also inhibited human GV sPLA₂ with similar potency, while it did not inhibit human GX sPLA₂. The elucidation of the stereoelectronic characteristics that affect the in vitro activity of these compounds was achieved by using a combination of simulated annealing to sample low-energy conformations before the docking procedure, and molecular docking calculations.

© 2011 Elsevier Ltd. All rights reserved.

1. Introduction

Phospholipase A₂ (PLA₂) is a superfamily of enzymes which are characterized by their ability to catalyze the hydrolysis of the *sn*-2 ester bond of glycerophospholipids releasing free fatty acids, including arachidonic acid, and lysophospholipids.¹ Arachidonic acid is supplied to the downstream cyclooxygenases COX-1 and COX-2, and to the 5-lipoxygenase for the production of eicosanoids,² while lysophospholipids, such as lysophosphatidic acid and lysophosphatidylcholine, and their metabolites, such as platelet activating factor, are potent bioactive mediators, acting through their cognate G-protein-coupled receptors.

Cytosolic PLA₂ (GIVA cPLA₂) plays an important role in inflammation. Various studies on transgenic mice lacking GIVA cPLA₂ showed a 90% reduction in the production of prostaglandins and leukotrienes.^{3,4} The biochemistry and the role of sPLA₂ enzymes have been recently reviewed by Lambeau and Gelb.⁵ The 10 known mammalian sPLA₂s are the groups: IB, IIA, IIC, IID, IIE, IIF, III, V, X and XI. Among the members of the mammalian sPLA₂ enzymes, the GIIA sPLA₂ is an interesting anti-inflammatory drug target because of its potential role in a number of different inflammatory diseases.⁵

GIIA sPLA₂ is a low molecular weight enzyme (14 kDa) with seven disulfide bonds, and was cloned in 1989.⁶ The crystal structure of the

enzyme reveals a highly conserved Ca²⁺-binding loop and a catalytic dyad consisting of His47/Asp91.^{7,8} The substrate hydrolysis proceeds through the activation of a water molecule by the catalytic histidine and subsequent attack of the *sn*-2 ester carbonyl carbon. Besides this histidine, there is an aspartate residue (Asp48), which together with the other residues of the Ca²⁺-binding loop (Gly29, Gly31 and His27), act as a ligand cage for the calcium ion. The crystal structure of GIIA sPLA₂ enzyme has also defined a conserved active site with a hydrophobic region lined near the N-terminal helix.^{7,8}

Since PLA₂ enzymes have been associated with various inflammatory diseases, the elucidation of their biological roles through the use of small synthetic inhibitors is of high importance. Most recently, Magrioti and Kokotos reviewed the various classes of PLA₂ inhibitors discussing their potential role as new anti-inflammatory agents.⁹ The design of novel GIIA sPLA₂ inhibitors may be accomplished using computational methods which are greatly aided by the availability of a number of GIIA sPLA₂ crystal structures with or without a ligand bound in the active site. Among the various reported crystal structures of the enzyme deposited in the RCSB protein data bank are the crystal structures with PDB IDs: 1DB4,¹⁰ 1DB5,¹⁰ 1J1A¹¹ and 1KVO.¹² However, the optimization of the activity of the GIIA sPLA₂ inhibitors, requires the better understanding of the receptor–ligand interactions and the development of a strategy to predict the inhibitory activity of new molecules. Techniques based on the field of computational chemistry are very helpful in this case. Previous computational research works on the GIIA sPLA₂ inhibitors include molecular docking cal-

* Corresponding author. Tel.: +30 2107274462; fax: +30 2107274761.

E-mail address: gkokotos@chem.uoa.gr (G. Kokotos).

culations,¹³ molecular dynamics simulations (MD)¹⁴ and three-dimensional quantitative structure–activity relationship (3D-QSAR) methodologies.^{15,16} Among these techniques molecular docking is a powerful technique, which contributes to the understanding of the stereoelectronic factors that affect the inhibitory activity of small molecules against a target receptor.^{17–19}

Recently, a novel class of GIVA cPLA₂ inhibitors, the 2-oxoamides (Fig. 1), has been developed.^{20–27} Long chain 2-oxoamides based on δ - and γ -amino acids ($m = 2$ and $m = 1$, respectively) are potent inhibitors of the GIVA cPLA₂ enzyme showing interesting in vivo anti-inflammatory and analgesic activity.^{21,25} Notably, such 2-oxoamides containing a free carboxyl group do not inhibit the other major intracellular PLA₂ enzyme, the Ca²⁺-independent GVIA iPLA₂,²⁴ although a cross-reactivity might be expected because both GIVA cPLA₂ and GVIA iPLA₂ enzymes are serine hydrolases and share a common catalytic mechanism. However, a few 2-oxoamides displayed some inhibition, although weak, of GV sPLA₂.²⁵

The aim of this work was to identify 2-oxoamides able to inhibit sPLA₂s. In the present report, the synthesis of new 2-oxoamides based on α -amino acids and the in vitro evaluation against three human sPLA₂s (GIIA, GV and GX sPLA₂) are described. To understand the binding mode of 2-oxoamides to GIIA sPLA₂, molecular docking calculations were performed.

2. Results and discussion

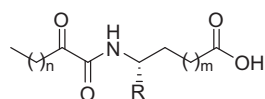
2.1. Synthesis of inhibitors

The synthesis of the new 2-oxoamides is depicted in Schemes 1 and 2. The methyl ester of (*S*)-leucine (**1a**) was coupled with 2-hydroxyhexadecanoic acid using 1-(3-dimethylaminopropyl)-3-ethyl carbodiimide (WSCl) as a condensing agent in the presence of 1-hydroxybenzotriazole (HOBT) (Scheme 1). After saponification of compound **2a**, oxidation of the 2-hydroxyamide **3a** was carried out by the NaOCl/AcNH-TEMPO method²¹ leading to the target compound **GK126**. Starting from the ethyl ester of (*R*)-leucine (**1b**), compound **GK145**, the enantiomer of **GK126** was prepared. Compound **GK144** was synthesized starting from the ethyl ester of (*S*)-leucine by coupling with hexadecanoic acid and subsequent saponification.

Compounds **GK111**, **GK112**, **GK122** and **GK141** were prepared by coupling 2-hydroxyhexadecanoic acid with *tert*-butyl glycinate (**4a**), β -alaninate (**4b**), δ -aminovalerate (**4c**) and (*S*)-phenylalaninate (**4d**), respectively (Scheme 2). Oxidation of 2-hydroxyamides **5a–d** was carried out by the Dess–Martin method,²⁸ followed by treatment of compounds **6a–d** with trifluoroacetic acid, to afford the target compounds. The synthesis of AX115 is described elsewhere.²⁶

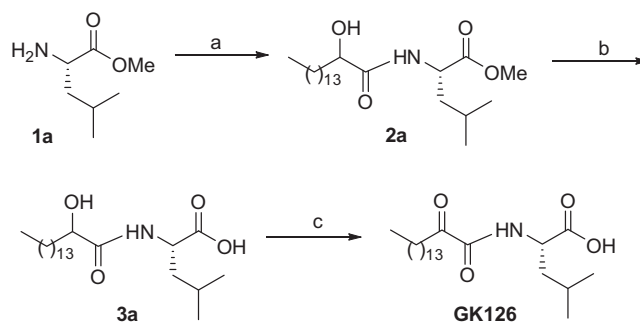
2.2. In vitro inhibition of GIIA sPLA₂, GV sPLA₂ and GX sPLA₂

The activity of compounds **GK111**, **GK112**, **GK122**, **GK126**, **GK141**, **GK144**, **GK145**, and **AX115** was studied against three different human enzymes using a continuous fluorimetric assay described previously.²⁹ The results for GIIA sPLA₂, GV sPLA₂ and GX sPLA₂ are summarized in Table 1. 2-Oxoamides **GK111**, **GK112** and **GK122**, based on glycine, β -alanine and δ -aminovaleric



$n = 8-12$, $m = 1, 2$, $R =$ short alkyl chain

Figure 1. General structure of 2-oxoamide inhibitors of GIVA cPLA₂.



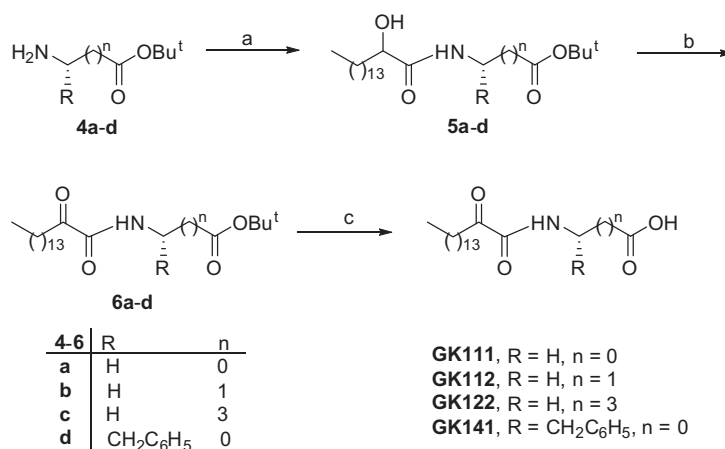
Scheme 1. Reagents and conditions: (a) CH₃(CH₂)₁₃CHOHCOOH, Et₃N, WSCI, HOBT, CH₂Cl₂; (b) 1 N NaOH, dioxane/H₂O 9:1; (c) NaOCl, AcNH-TEMPO, NaBr, NaHCO₃, EtOAc/PhCH₃/H₂O 3:3:0.5, 0 °C.

acid, respectively, inhibited GIIA sPLA₂ in the micromolar range (IC₅₀ 4.20–11.67 μ M). At 16.6 μ M concentration, none of them showed any significant inhibition of GV sPLA₂ and GX sPLA₂. It seems that for the inhibition of GIIA sPLA₂, the optimum distance between the 2-oxoamide group and the carboxyl group corresponds to one carbon atom. Increasing the length leads to less potent inhibitors. Comparing the results for **GK111** and **AX115**, it was obvious that a free carboxyl group was necessary for the inhibition of GIIA sPLA₂. The introduction of a side chain corresponding to leucine increased the inhibitory activity for GIIA sPLA₂ by an order of magnitude. **GK126** inhibited GIIA sPLA₂ with an IC₅₀ value of 0.30 μ M. This 2-oxoamide also inhibited GV sPLA₂ at the same level (IC₅₀ 0.44 μ M), while it did not show any inhibition of GX sPLA₂. The inhibitory activity of **GK126** was also measured against the corresponding mouse enzymes. Similar IC₅₀ values for mouse GIIA sPLA₂ and GV sPLA₂ were found (0.18 μ M and 2.60 μ M, respectively). Compound **GK145**, based on (*R*)-leucine, displayed six times lower potency for GIIA sPLA₂ and four times lower potency for GV sPLA₂, indicating that the (*S*)-configuration of the α -amino acid makes more favorable contacts with the enzyme active site. Replacement of either the 2-oxoamide functionality of **GK126** by an amide functionality (**GK144**) or the side chain by a chain corresponding to phenylalanine (**GK141**) led to inactive compounds. The most potent inhibitor against sPLA₂ (**GK126**) did not present any significant inhibition against cPLA₂ (not higher than 12% inhibition at 1 μ M). Thus, we identified a 2-oxoamide based on the natural α -amino acid leucine, which displayed submicromolar inhibition of GIIA sPLA₂.

2.3. Molecular docking calculations

The 2-oxoamide inhibitors were initially designed to interact with the hydroxyl group of the active site serine of GIVA cPLA₂.²⁰ Recently, the location of the 2-oxoamide inhibitor AX007 within the active site of GIVA cPLA₂ was determined by a combination of molecular dynamics and deuterium exchange mass spectrometry.³⁰ However, the binding mode of 2-oxoamides with GIIA sPLA₂ is not obvious because GIIA sPLA₂ is not a serine hydrolase and it utilizes a different catalytic mechanism than GIVA cPLA₂. Thus, to understand how the 2-oxoamides interact with GIIA sPLA₂, we decided to perform molecular docking calculations. Four 2-oxoamide inhibitors based on α -amino acids, **GK126**, **GK145**, **GK111** and **GK141**, were selected for this study. The molecular docking calculations were performed using the genetic docking algorithm GOLD 4.1.^{31–33}

The active site of GIIA sPLA₂ consists of a hydrophilic region and a hydrophobic region. The hydrophilic region, where catalytic activity occurs, is formed by the residues His47 and Asp91, and by the Ca²⁺-binding loop. The Ca²⁺-binding loop consists of the residues Gly29, Gly31, His27 and Asp48. The calcium ion is



Scheme 2. Reagents and conditions: (a) CH₃(CH₂)₁₃CHOHCOOH, Et₃N, WSCI, HOBT, CH₂Cl₂; (b) Dess–Martin reagent, CH₂Cl₂; (c) 50% TFA/CH₂Cl₂.

Table 1
In vitro inhibition of the enzymatic activity of human GIIA, GV and GX sPLA₂s by 2-oxoamides

Code	Structure	IC ₅₀ (μM)		
		hGIIA sPLA ₂	hGV sPLA ₂	hGX sPLA ₂
GK111		4.20 ± 0.20	43% ^a	23% ^a
GK112		5.60 ± 0.25	47% ^a	18% ^a
GK122		11.67 ± 0.50	49% ^a	7% ^a
AX115		3% ^a	9% ^a	22% ^a
GK126		0.30 ± 0.06 (0.18 ± 0.04) ^b	0.44 ± 0.04 (2.60 ± 0.33) ^c	50% ^a (58% ^a) ^d
GK145		1.75 ± 0.07	1.50 ± 0.23	>1.66
GK144		>1.66	>1.66	>1.66
GK141		>1.66	>1.66	>1.66

^a At 16.6 μM concentration.

^b For mouse GIIA sPLA₂.

^c For mouse GV sPLA₂.

^d For mouse GX sPLA₂.

hepta-coordinated with a pentagonal bipyramidal geometry providing two binding sites for the substrate or the inhibitor.³⁴ The hydrophobic region, which binds the fatty acid tails of the sub-

strate, is formed by aliphatic and aromatic residues within or closed to the N-terminal helix, including Leu2, Phe5, Ile9, Ala17, Ala18, Tyr21 and Phe98.

Four GIIA sPLA₂ inhibitor X-ray structures have been selected in order to test if GOLD 4.1 is able to reproduce experimental crystallographic data (see Table 1 in Supplementary data).^{10–12} For each inhibitor, the best score pose has been selected to compare with the crystallographic one. The RMSD values after the superimposition of the crystallographic conformation and the conformation predicted by GOLD are smaller or equal to 1.0 Å, indicating that the two conformations are almost identical. Thus, the main interactions of each inhibitor with the GIIA sPLA₂ active site, reported in the literature,^{10–12} were reproduced by GOLD.

Six inhibitors (Table 2) have been chosen for the molecular docking studies since they possess a wide variety of biological activity. The high flexibility of the molecules imposed the use of a conformational sampling in an attempt to obtain low-energy conformers and to avoid false positives.³⁵ For this purpose the simulated annealing module in the SYBYL 8.0 molecular modeling package³⁶ was used in order to generate 100 annealed structures for each inhibitor, before the docking procedure. The annealed structures have subsequently been docked in the enzyme active site using GOLD. For each inhibitor the best score pose was chosen as the one that represents better the putative bioactive conformation. The docking results are summarized in Table 2. A good correlation between the IC₅₀ values and the GOLDScore Fitness values ($r^2 = 0.798$, $N = 5$) was observed. Five inhibitors with an experimentally determined IC₅₀ value have been used for the correlation procedure. However, the present study has focused on 2-oxoamides which are based on α -amino acids (GK126, GK145, GK111 and GK141). The most active inhibitor GK126 is scored with the highest GOLDScore Fitness. The inhibitor GK145, which is the (*R*)-enantiomer of GK126, shows both a higher IC₅₀ value against GIIA sPLA₂ and a lower GOLDScore Fitness than the inhibitor GK126. The GK111 inhibitor displays a higher IC₅₀ value and a lower GOLDScore Fitness than those of the inhibitors GK126 and GK145. The

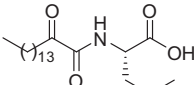
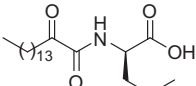
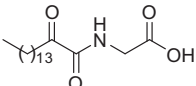
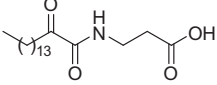
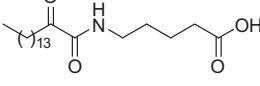
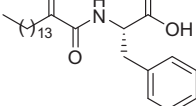
lowest GOLDScore Fitness was obtained for inhibitor GK141, which also showed the lowest inhibition against GIIA sPLA₂.

Using GOLD, the inhibitor–enzyme complexes were calculated and, it was possible to understand the main stereoelectronic characteristics that affect the inhibition of these compounds. Figure 2 presents the binding of the inhibitor GK126 in the GIIA sPLA₂ active site. The 2-oxoamide group participates in two hydrogen bonds with Gly29. The 2-carbonyl group participates in a hydrogen bond with the N–H of Gly29 (C=O···H–N 2.50 Å, O···N 3.30 Å) and the N–H of the 2-oxoamide group forms a hydrogen bond with the carbonyl group of Gly29 (N–H···O=C 1.65 Å, N···O 2.65). The 2-carbonyl group also interacts with the calcium ion (NHCOCO···Ca²⁺ 2.40 Å). The carboxylate group of the inhibitor interacts with the calcium ion (COO···Ca²⁺ 2.87 Å) and is involved in a hydrogen bond with Lys62 through a water molecule placed near the hydrophilic region of the active site (O···H–OH 1.94 Å, O···O 2.90 Å and H₂O···H–N 1.89 Å, O···N 2.89 Å). The side chain of (*S*)-leucine is in a suitable orientation to interact with Leu2 of the active site in aliphatic/aliphatic interactions. The long aliphatic 2-oxoacyl chain is accommodated in the hydrophobic region of the active site and participates in aliphatic/aliphatic and in aliphatic/aromatic interactions with residues Val3, Phe5, His6, Ile9, Ala17 and Phe98.

As aforementioned, the inhibitor GK145 is the (*R*)-enantiomer of the inhibitor GK126. According to the GK145–GIIA sPLA₂ complex calculated by GOLD (Fig. 3) the amide carbonyl of the 2-oxoamide group interacts with the calcium ion (NHCO···Ca²⁺ 2.30 Å). With regards to the inhibitor GK145, the 2-oxoamide group is flipped in comparison with that of GK126. As a result, the two hydrogen bonds with Gly29, in which participates the 2-oxoamide functionality of GK126, are not observed upon binding of GK145. This may be the reason that the inhibitor GK145 generates a lower GOLDScore Fitness and a higher IC₅₀ value against GIIA sPLA₂. On the other hand, the carboxylate group of the inhibitor interacts with the calcium ion (COO···Ca²⁺ 2.65 Å), but does not participate in the hydrogen bond with Lys62 through the water molecule. Instead of the hydrogen bond with Lys62, a hydrogen bond of the carboxylate group with a water molecule near the hydrophilic region of the active site is observed. The side chain of (*R*)-leucine is placed near Leu2 of the active site and interacts in a similar mode as the (*S*)-leucine of inhibitor GK126. The long aliphatic 2-oxoacyl chain is accommodated in the hydrophobic region and interacts with the residues Val3, Phe5, His6, Ile9, Ala17 and Phe98 in a similar mode as the one of the enantiomeric GK126.

The inhibitor GK111 is based on the α -amino acid glycine. The binding of GK111 in the GIIA sPLA₂ active site (Fig. 4) reveals an

Table 2
The GOLDScore Fitness for the GIIA sPLA₂ 2-oxoamide inhibitors based on the α -amino acids

Compound	Structure	IC ₅₀ (μ M)	Gsc. Fit.
GK126 (<i>S</i>)-Leu		0.30 \pm 0.06	85.91
GK145 (<i>R</i>)-Leu		1.75 \pm 0.07	84.91
GK111 Gly		4.20 \pm 0.20	78.89
GK112		5.60 \pm 0.25	77.33
GK122		11.67 \pm 0.50	75.69
GK141 (<i>S</i>)-Phe		>1.66	73.09

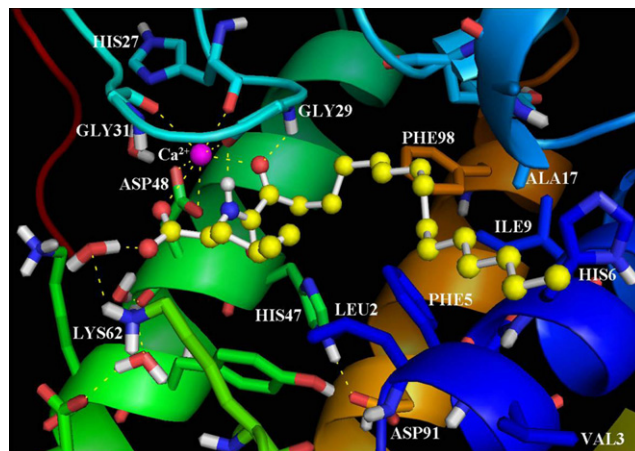


Figure 2. The binding mode of the inhibitor GK126 in the GIIA sPLA₂ active site as calculated using GOLD.

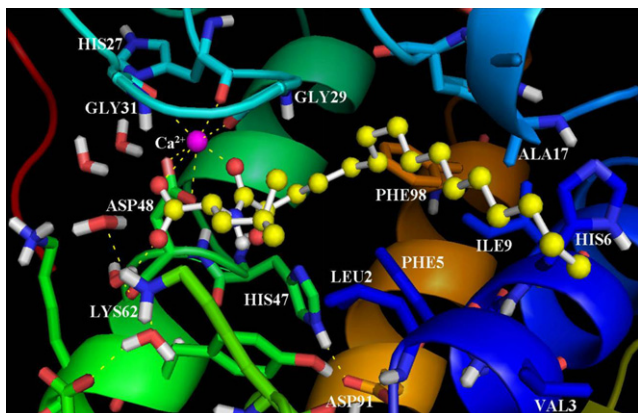


Figure 3. The binding mode of the inhibitor **GK145** in the GIIA sPLA₂ active site as calculated using GOLD.

interaction of the 2-carbonyl group of the inhibitor with the calcium ion ($\text{NHCOO} \cdots \text{Ca}^{2+}$ 2.70 Å). The carboxylate group interacts with the calcium ion ($\text{COO}^- \cdots \text{Ca}^{2+}$ 2.90 Å) and participates in two hydrogen bonds with Gly31 ($\text{COO}^- \cdots \text{H-N}$ 2.40 Å, $\text{O} \cdots \text{N}$ 3.40 Å) and Lys62 through a water molecule ($\text{O} \cdots \text{H-OH}$ 1.91 Å, $\text{O} \cdots \text{O}$ 2.89 Å and $\text{H}_2\text{O} \cdots \text{H-N}$ 1.89 Å, $\text{O} \cdots \text{N}$ 2.89 Å). In comparison with the binding of the inhibitor **GK126**, the two hydrogen bonds of the 2-oxoamide group with Gly29 are not observed. The lack of the (*S*)-leucine side chain, which interacts with Leu2 of the active site, also reduces the GOLDscore Fitness and increases the IC₅₀ value against GIIA sPLA₂. The long aliphatic 2-oxoacyl chain interacts with the residues Phe5, His6, Ile9, Ala17 and Phe98.

The binding of the inhibitor **GK141** (Fig. 5), which is based on the α -amino acid (*S*)-phenylalanine, indicates a hydrogen bond of the N–H of the 2-oxoamide group with Gly29 ($\text{N-H} \cdots \text{O}$ 1.97 Å, $\text{N} \cdots \text{O}$ 2.98 Å). The 2-carbonyl group of the inhibitor interacts with the calcium ion ($\text{NHCOO} \cdots \text{Ca}^{2+}$ 2.60 Å). The carboxylate group interacts with the calcium ion ($\text{COO}^- \cdots \text{Ca}^{2+}$ 2.64 Å) and participates in two hydrogen bonds with Gly31 ($\text{COO}^- \cdots \text{H-N}$ 1.67 Å, $\text{O} \cdots \text{N}$ 2.60 Å) and with Lys62 through a water molecule ($\text{O} \cdots \text{H-OH}$ 1.60 Å, $\text{O} \cdots \text{O}$ 2.56 Å and $\text{H}_2\text{O} \cdots \text{H-N}$ 1.89 Å, $\text{O} \cdots \text{N}$ 2.89 Å). The 2-carbonyl group of **GK141** does not participate in the hydrogen bond with Gly29 as the one of the inhibitor **GK126**. The side chain of (*S*)-Phe seems to participate in aromatic/aliphatic and aromatic (π - π) stacking interactions with Leu2, Phe5, Tyr51 and His47. On the

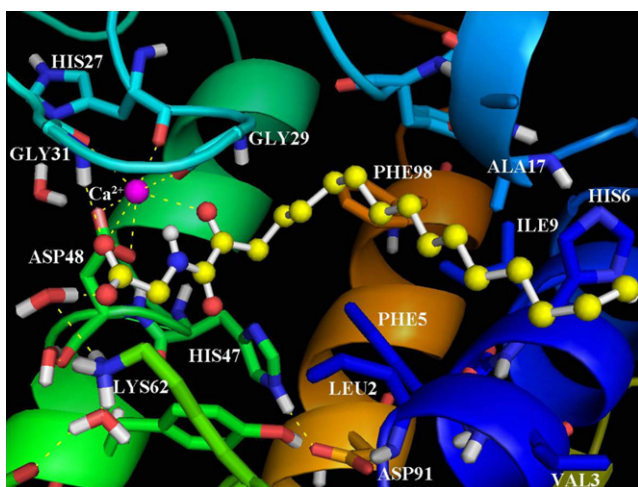


Figure 4. The binding mode of the inhibitor **GK111** in the GIIA sPLA₂ active site as calculated using GOLD.

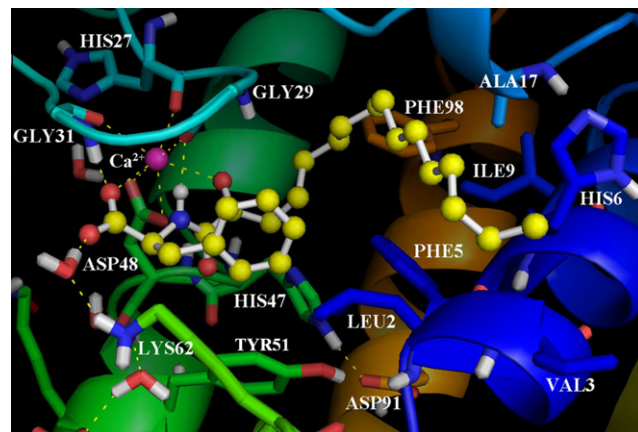


Figure 5. The binding mode of the inhibitor **GK141** in the GIIA sPLA₂ active site as calculated using GOLD.

other hand, the region around the side chain of (*S*)-phenylalanine seems to be narrow and perhaps the phenyl ring clashes with the aforementioned residues; this may be the reason that **GK141** gives the lowest GOLDscore Fitness among the studied 2-oxoamide inhibitors. The long aliphatic 2-oxoacyl chain participates in aliphatic/aliphatic and aliphatic/aromatic interactions with residues including Phe5, His6, Ile9 and Phe98.

Based on the molecular docking studies, it was possible to understand the structural characteristics that contribute to the enhancement of the inhibitory activity of the 2-oxoamide **GK126** (Fig. 6). The 2-oxoamide group is essential for the binding because it participates in hydrogen bonds with Gly29 and interacts with the calcium ion. The (*R*)-enantiomer displays a lower GOLDscore and a higher IC₅₀ value, because the 2-oxoamide functionality is flipped and does not engage in hydrogen bonding with Gly29. The carboxylate group is also essential for binding because interacts with the calcium ion and participates in a hydrogen bond with Lys62 through a water molecule placed near the hydrophilic region of the active site. The (*S*)-leucine side chain contributes to the tight binding of **GK126** by interacting with the side chain of the active site Leu2. The inhibitor **GK111** lacks the (*S*)-leucine side chain and as a consequence its inhibitory activity is decreased. The long 2-oxoacyl aliphatic chain contributes to the tight binding by interacting with the hydrophobic region of the active site (Val3, Phe5, His6, Ile9, Ala17 and Phe98).

A variety of sPLA₂ inhibitors have been reported in the literature.^{5,9,37} Gelb et al. have studied various inhibitors for their selectivity over the complete set of human and mouse sPLA₂s (groups I,

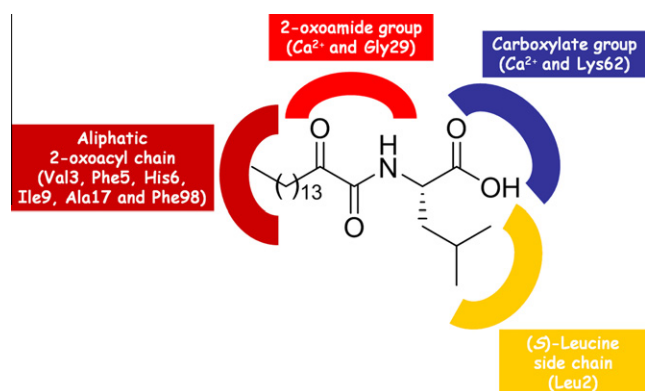


Figure 6. The pharmacophore segments of the inhibitor **GK126** and their interactions with the surrounding amino acids and the calcium ion of the active site.

II, V, X, and XIII sPLA₂).³⁸ They have reported a highly potent and selective indole-based inhibitor of GX sPLA₂, specific inhibitors for GIIA and GIIE sPLA₂ and a substituted 6,7-benzoinidole that inhibits nearly all human and mouse sPLA₂s in the low nanomolar range.³⁹ In recent years, interest in sPLA₂ inhibitors has increased because they seem to play an important role in the prevention of atherosclerotic cardiovascular disease.^{40,41} In the present work, we demonstrate that a new 2-oxoamide is able to inhibit human GIIA sPLA₂ in the submicromolar range and the mode of its interaction with the GIIA sPLA₂ has been studied using molecular docking. These data indicate that this compound constitutes a new lead for the development of new GIIA sPLA₂ inhibitors.

3. Conclusion

2-Oxoamide derivatives based on α -amino acids have been synthesized and tested for their in vitro inhibitory activity against three human sPLA₂s (GIIA, GV and GX). Compound **GK126**, which is based on (S)-leucine, displayed inhibition of human and mouse GIIA sPLA₂ (IC₅₀ 300 nM and 180 nM, respectively). It also inhibited the human GV sPLA₂ with similar potency, while it did not display any measurable inhibition of GX sPLA₂. Using a combination of simulated annealing and molecular docking calculations, it was possible to explore the inhibitor–enzyme complexes and rationalize the stereoelectronic characteristics that affect the inhibition potency of these compounds. The annealed structures resulted from the investigation of the conformational space of each inhibitor were docked in the enzyme active site. Inhibitor **GK126**, which is the most active compound among the inhibitors tested, is scored with the highest GOLDscore Fitness. The 2-oxoamide functionality is essential for the binding by interacting with the calcium ion and by participating in two hydrogen bonds with Gly29.

4. Experimental

4.1. Chemistry

Melting points were determined on a Buchi 530 apparatus and are uncorrected. Specific rotations were measured on a Perkin–Elmer 343 polarimeter using a 10 cm cell. NMR spectra were recorded on a Varian Mercury spectrometer. ¹H and ¹³C NMR spectra were recorded at 200 MHz and 50 MHz, respectively in CDCl₃ or as specified. Chemical shifts are given in ppm, and peak multiplicities are described as follows: s, singlet, d, doublet, t, triplet and m, multiplet. Electron spray ionization (ESI) mass spectra were recorded on a Finnigan, Surveyor MSQ Plus spectrometer. TLC plates (Silica Gel 60 F254) and Silica Gel 60 (70–230 or 230–400 mesh) for column chromatography were purchased from Merck. Spots were visualised with UV light and/or phosphomolybdic acid and/or ninhydrin, both in EtOH. Dichloromethane was dried by standard procedures and stored over molecular sieves. All other solvents and chemicals were reagent grade and used without further purification.

The synthesis of inhibitor **AX115** and of compounds **5a–c** and **6a–c** has been described elsewhere.²⁶

4.2. Synthesis of the 2-oxoamide inhibitors

4.2.1. General method for the coupling of 2-hydroxyhexadecanoic acid with amino components

To a stirred solution of 2-hydroxyhexadecanoic acid (1.0 mmol) and hydrochloride amino component (1.0 mmol) in CH₂Cl₂ (10 mL), Et₃N (0.3 mL, 2.2 mmol) and subsequently 1-(3-dimethylaminopropyl)-3-ethyl carbodiimide hydrochloride (WSCl) (0.21 g, 1.1 mmol) and 1-hydroxybenzotriazole (HOBt) (0.14 g, 1.0 mmol)

were added at 0 °C. The reaction mixture was stirred for 1 h at 0 °C and overnight at room temperature. The solvent was evaporated under reduced pressure and EtOAc (20 mL) was added. The organic layer was washed consecutively with brine, 1 N HCl, brine, 5% NaHCO₃, and brine, dried over Na₂SO₄ and evaporated under reduced pressure. The residue was purified by column chromatography using CH₂Cl₂/MeOH 99:1 as eluent.

4.2.1.1. (2S)-Methyl 2-(2-hydroxyhexadecanamido)-4-methylpentanoate (2a). Yield 79%; white solid; mp 47–49 °C; ¹H NMR (200 MHz, CDCl₃): δ 7.02–6.82 (m, 1H), 4.70–4.55 (m, 1H), 4.20–4.10 (m, 1H), 3.73 (s, 3H), 3.07 (s, 1H), 1.81–1.53 (m, 5H), 1.39–1.24 (m, 24H), 0.89 (m, 9H); ¹³C NMR (50 MHz, CDCl₃): δ 174.15, 173.91, 72.05, 52.30, 50.27, 41.40, 34.74, 34.64, 31.89, 29.66, 29.63, 29.54, 29.36, 29.33, 24.82, 22.80, 22.66, 21.76, 21.67, 14.09. Anal. Calcd for C₂₃H₄₅NO₄: C, 69.13; H, 11.35; N, 3.51. Found: C, 68.99; H, 11.48; N, 3.59.

4.2.1.2. (2R)-Ethyl 2-(2-hydroxyhexadecanamido)-4-methylpentanoate (2b). Yield 64%; white solid; mp 34–35 °C; ¹H NMR (200 MHz, CDCl₃): δ 7.00–6.90 (m, 1H), 4.60–4.55 (m, 1H), 4.15–4.00 (m, 3H), 1.78–1.58 (m, 6H), 1.41–1.22 (m, 27H), 0.90 (m, 9H); ¹³C NMR (50 MHz, CDCl₃): δ 174.27, 173.27, 72.08, 61.37, 50.37, 41.44, 34.74, 34.64, 31.86, 29.63, 29.52, 29.37, 29.29, 24.88, 24.83, 22.79, 22.62, 21.80, 21.71, 14.03. Anal. Calcd for C₂₄H₄₇NO₄: C, 69.69; H, 11.45; N, 3.39. Found: C, 69.57; H, 11.56; N, 3.44.

4.2.1.3. (S)-Ethyl 4-methyl-2-palmitamidopentanoate. Yield 79%; white solid; mp 51–52 °C; ¹H NMR (200 MHz, CDCl₃): δ 6.00 (d, *J* = 8.4 Hz, 1H), 4.67–4.52 (m, 1H), 4.15 (q, *J* = 7.1 Hz, 2H), 2.18 (t, *J* = 7.5 Hz, 2H), 1.57 (m, 5H), 1.24 (m, 27H), 1.00–0.85 (m, 9H); ¹³C NMR (50 MHz, CDCl₃): δ 173.25, 172.83, 61.12, 50.51, 41.71, 36.47, 31.83, 29.59, 29.56, 29.51, 29.41, 29.26, 29.14, 25.54, 24.80, 22.72, 22.58, 21.91, 14.03, 14.00. Anal. Calcd for C₂₄H₄₇NO₃: C, 72.49; H, 11.91; N, 3.52. Found: C, 72.34; H, 12.09; N, 3.41.

4.2.1.4. (2S)-tert-Butyl 2-(2-hydroxyhexadecanamido)-3-phenylpropanoate (5d). Yield 57%; white solid; mp 55–56 °C; ¹H NMR (200 MHz, CDCl₃): δ 7.30–7.20 (m, 5H, Ar), 4.80–4.68 (m, 1H), 4.07–4.01 (m, 1H), 3.15–2.97 (m, 2H), 1.80–1.46 (m, 2H), 1.37 (s, 9H), 1.23 (s, 24H), 0.84 (t, *J* = 6.7 Hz, 3H); ¹³C NMR (50 MHz, CDCl₃): δ 173.60, 170.63, 135.78, 129.09, 128.03, 126.61, 82.13, 71.74, 52.90, 37.87, 34.47, 31.59, 29.37, 29.22, 29.12, 29.04, 27.57, 24.61, 22.36, 13.80; MS (ESI) *m/z* (%): (48) 476.3 (M+H)⁺, 420.3 (100) (M⁻Bu+H+H)⁺. Anal. Calcd for C₂₉H₄₉NO₄: C, 73.22; H, 10.38; N, 2.94. Found: C, 73.05; H, 10.46; N, 3.04.

4.2.2. General method for the saponification of 2-hydroxyamides

To a stirred solution of a 2-hydroxyamide ester (1.0 mmol) in a mixture of dioxane–H₂O (9:1, 10 mL) was added 1 N NaOH (1.1 mL, 1.1 mmol), and the mixture was stirred for 12 h at room temperature. The organic solvent was evaporated under reduced pressure, and H₂O (5 mL) was added. The aqueous layer was washed with EtOAc, acidified with 1 N HCl, and extracted with EtOAc (3 × 6 mL). The combined organic layers were washed with brine, dried over Na₂SO₄, and evaporated under reduced pressure.

4.2.2.1. (2S)-2-(2-Hydroxyhexadecanamido)-4-methylpentanoic acid (3a). Yield 89%; white solid; ¹H NMR (200 MHz, CDCl₃): δ 7.80 (br s, 1H), 7.40–7.30 (m, 1H), 4.44 (m, 1H), 4.08 (m, 1H), 1.80–1.50 (m, 6H), 1.45–1.10 (m, 24H), 0.89 (m, 9H); ¹³C NMR (50 MHz, CDCl₃): δ 176.59, 175.40, 72.19, 71.98, 51.21, 40.56, 40.39, 34.47, 31.95, 29.74, 29.68, 29.48, 29.37, 25.27, 25.15, 24.97, 23.02,

22.68, 21.44, 21.26, 14.10. Anal. Calcd for C₂₂H₄₃NO₄: C, 68.53; H, 11.24; N, 3.63. Found: C, 68.41; H, 11.42; N, 3.51.

4.2.2.2. (2R)-2-(2-Hydroxyhexadecanamido)-4-methylpentanoic acid (3b). Yield 54%; white solid; ¹H NMR (200 MHz, CDCl₃): δ 7.80 (br s, 1H), 7.40–7.30 (m, 1H), 4.46 (m, 1H), 4.07 (m, 1H), 1.80–1.50 (m, 6H), 1.45–1.10 (m, 24H), 0.89 (m, 9H); ¹³C NMR (50 MHz, CDCl₃): δ 176.57, 175.38, 72.20, 71.98, 51.15, 40.55, 40.37, 34.45, 31.92, 29.73, 29.67, 29.47, 29.36, 25.26, 25.13, 24.96, 23.02, 22.67, 21.43, 21.25, 14.09. Anal. Calcd for C₂₂H₄₃NO₄: C, 68.53; H, 11.24; N, 3.63. Found: 68.43; H, 11.32; N, 3.51.

4.2.2.3. (S)-4-Methyl-2-palmitamidopentanoic acid (GK144). Yield: 100%; white solid; mp 93–95 °C; ¹H NMR (200 MHz, CDCl₃): δ 10.46 (s, 1H), 6.22 (d, *J* = 8.2 Hz, 1H), 4.70–4.55 (m, 1H), 2.24 (t, *J* = 7.6 Hz, 2H), 1.80–1.45 (m, 5H), 1.40–1.10 (m, 24H), 1.00–0.85 (m, 9H); ¹³C NMR (50 MHz, CDCl₃): δ 176.47, 174.23, 50.83, 41.24, 36.44, 31.89, 29.66, 29.48, 29.32, 29.18, 25.63, 24.86, 22.79, 22.64, 21.85, 14.06. Anal. Calcd for C₂₂H₄₃NO₃: C, 71.50; H, 11.73; N, 3.79. Found: C, 71.31; H, 11.89; N, 3.70.

4.2.3. General method for the oxidation of 2-hydroxyamides (Method A)

To a solution of 2-hydroxyamide (1.0 mmol) in a mixture of toluene (3 mL) and EtOAc (3 mL), a solution of NaBr (0.11 g, 1.1 mmol) in water (0.5 mL) was added followed by AcNH-TEMPO (2.2 mg, 0.01 mmol). To the resulting biphasic system, which was cooled at 0 °C, an aqueous solution of 0.35 M NaOCl (3.1 mL, 1.1 mmol) containing NaHCO₃ (0.25 g, 3 mmol) was added dropwise under vigorous stirring, at 0 °C over a period of 1 h. After the mixture had been stirred for a further 15 min at 0 °C, EtOAc (10 mL) and H₂O (10 mL) were added. The aqueous layer was separated and washed with EtOAc (2 × 10 mL). The combined organic layers were washed consecutively with 5% aqueous citric acid (10 mL) containing KI (0.04 g), 10% aqueous Na₂S₂O₃ (10 mL), and brine and dried over Na₂SO₄. The solvents were evaporated under reduced pressure and the residue was purified by column chromatography using petroleum ether (bp 40–60 °C)/EtOAc 2:8 as eluent.

4.2.3.1. (S)-4-Methyl-2-(2-oxohexadecanamido)pentanoic acid (GK126). Yield 29%; yellow oil; ¹H NMR (200 MHz, CDCl₃): δ 7.46 (m, 1H), 4.51 (m, 1H), 2.91 (t, *J* = 7.0 Hz, 2H), 1.80–1.40 (m, 5H), 1.40–1.10 (m, 22H), 0.90 (m, 9H); ¹³C NMR (50 MHz, CDCl₃): δ 198.68, 170.47, 160.36, 51.40, 40.83, 36.87, 31.91, 29.68, 29.49, 29.42, 29.36, 29.08, 24.86, 23.07, 22.92, 22.67, 21.53, 14.09; MS (ESI) *m/z* (%): 384.3 (M+H)⁺. Anal. Calcd for C₂₂H₄₁NO₄: C, 68.89; H, 10.77; N, 3.65. Found: C, 68.75; H, 10.89; N, 3.75.

4.2.3.2. (R)-4-Methyl-2-(2-oxohexadecanamido)pentanoic acid (GK145). Yield 35%; yellow oil; ¹H NMR (200 MHz, CDCl₃): δ 7.38 (m, 1H), 4.56 (m, 1H), 2.91 (t, *J* = 7.0 Hz, 2H), 1.80–1.45 (m, 5H), 1.40–1.10 (m, 22H), 0.90 (m, 9H); ¹³C NMR (50 MHz, CDCl₃): δ 198.58, 177.46, 160.29, 51.18, 40.82, 36.85, 34.74, 31.90, 29.67, 29.47, 29.40, 29.34, 29.05, 28.87, 27.27, 24.85, 23.05, 22.88, 22.66, 21.50, 14.09; MS (ESI) *m/z* (%): 384.3 (M+H)⁺. Anal. Calcd for C₂₂H₄₁NO₄: C, 68.89; H, 10.77; N, 3.65. Found: C, 68.72; H, 10.89; N, 3.76.

4.2.4. General method for the oxidation of 2-hydroxyamides (Method B)

To a solution of 2-hydroxyamide (1.0 mmol) in dry CH₂Cl₂ (10 mL) Dess–Martin periodinane was added (0.64 g, 1.5 mmol) and the mixture was stirred for 1 h at room temperature. The organic solvent was evaporated under reduce pressure and Et₂O

(30 mL) was added. The organic phase was washed with saturated aqueous NaHCO₃ (20 mL) containing Na₂S₂O₃ (1.5 g, 9.5 mmol), H₂O (20 mL), dried over Na₂SO₄ and the organic solvent was evaporated under reduced pressure. The residue was purified by column chromatography using petroleum ether (bp 40–60 °C)/EtOAc 9:1 as eluent.

4.2.4.1. (S)-tert-Butyl 2-(2-oxohexadecanamido)-3-phenylpropanoate (6d). Yield 63%; white solid; mp 46–47 °C; [α]_D = +29.0 (c 1, CH₂Cl₂); ¹H NMR (200 MHz, CDCl₃): δ 7.34 (d, *J* = 8.4 Hz, 1H) 7.30–7.08 (m, 5H Ar), 4.72–4.62 (m, 1H), 3.08 (d, *J* = 6.3 Hz, 2H), 2.84 (t, *J* = 7.3 Hz, 2H), 1.62–1.45 (m, 2H), 1.37 (s, 9H), 1.23 (s, 22H), 0.84 (t, *J* = 6.7 Hz, 3H); ¹³C NMR (50 MHz, CDCl₃): δ 198.23, 169.48, 159.45, 135.61, 129.25, 128.35, 126.97, 82.45, 53.49, 37.96, 36.56, 31.81, 29.54, 29.48, 29.32, 29.25, 29.21, 28.93, 27.77, 23.06, 22.58, 14.01; MS (ESI) *m/z* (%): 472.5 (M–H)[–]. Anal. Calcd for C₂₉H₄₇NO₄: C, 73.53; H, 10.00; N, 2.96. Found: C, 73.41; H, 10.16; N, 3.09.

4.2.5. General method for the cleavage of tert-butyl ester

A solution of the *tert*-butyl ester derivative (1 mmol) in 50% TFA/CH₂Cl₂ (0.5 M) was stirred for 1 h at room temperature. The organic solvent was evaporated under reduced pressure. The residue was purified by recrystallization [EtOAc/petroleum ether (bp 40–60 °C)].

4.2.5.1. 2-(2-Oxohexadecanamido)acetic acid (GK111). Yield 90%; white solid; ¹H NMR (200 MHz, CDCl₃): δ 5.00 (m, 1H), 3.95 (d, *J* = 4.0 Hz, 2H), 2.85 (t, *J* = 7.0 Hz, 2H), 1.80–1.50 (m, 4H), 1.40–1.15 (m, 20H), 0.90 (m, 3H); ¹³C NMR (50 MHz, CD₃OD): δ 197.85, 172.79, 161.34, 40.44, 40.30, 38.31, 36.58, 31.91, 29.61, 29.44, 29.37, 29.32, 29.01, 23.20, 23.07, 22.57, 13.30; MS (ESI) *m/z* (%): 326.4 (M–H)[–]. Anal. Calcd for C₁₈H₃₃NO₄: C, 66.02; H, 10.16; N, 4.28. Found: C, 65.89; H, 10.34; N, 4.15.

4.2.5.2. 3-(2-Oxohexadecanamido)propanoic acid (GK112). Yield 75%; white solid; ¹H NMR (200 MHz, CDCl₃): δ 4.90 (b, 1H), 3.48 (t, *J* = 7.0 Hz, 2H), 2.82 (t, *J* = 7.2 Hz, 2H), 2.54 (t, *J* = 7.0 Hz, 2H), 1.62–1.55 (m, 2H), 1.50–1.05 (m, 22H), 0.88 (t, *J* = 7.0 Hz, 3H); ¹³C NMR (50 MHz, CDCl₃): δ 198.32, 173.91, 160.26, 38.17, 36.59, 34.94, 33.35, 32.98, 31.91, 29.61, 29.42, 29.32, 29.02, 23.36, 23.11, 22.57, 13.29; MS (ESI) *m/z* (%): 340.3 (100) [M–H][–]. Anal. Calcd for C₁₉H₃₅NO₄: C, 66.83; H, 10.33; N, 4.10. Found: C, 66.68; H, 10.48; N, 4.19.

4.2.5.3. 5-(2-Oxohexadecanamido)pentanoic acid (GK122). Yield 91%; white solid; mp 103–105 °C; ¹H NMR (200 MHz, CDCl₃): δ 7.06 (t, *J* = 5.6 Hz, 1H), 3.39–3.26 (m, 2H), 2.91 (t, *J* = 7.4 Hz, 2H), 2.40 (t, *J* = 7.0 Hz, 2H), 1.78–1.48 (m, 6H), 1.26 (s, 22H), 0.88 (t, *J* = 6.6 Hz, 3H); ¹³C NMR (50 MHz, CDCl₃): δ 199.34, 178.56, 160.27, 38.83, 36.73, 33.27, 31.89, 29.62, 29.57, 29.42, 29.32, 29.04, 28.58, 23.16, 22.66, 21.79, 14.09; MS (ESI) *m/z* (%): 368.3 (100) [M–H][–]. Anal. Calcd for C₂₁H₃₉NO₄: C, 68.25; H, 10.64; N, 3.79. Found: C, 68.11; H, 10.80; N, 3.84.

4.2.5.4. (S)-2-(2-Oxohexadecanamido)-3-phenylpropanoic acid (GK141). Yield 95%; white solid; mp 104–105 °C; [α]_D = +8.7 (c 1, CH₃OH); ¹H NMR (200 MHz, CD₃OD): δ 7.31–7.15 (m, 5H Ar), 4.72–4.64 (m, 1H), 3.26–3.23 (m, 1H), 3.12–2.96 (m, 2H), 2.75 (t, *J* = 7.0 Hz, 2H), 1.59–1.46 (m, 2H), 1.29 (s, 22H), 0.90 (t, *J* = 6.7 Hz, 3H); ¹³C NMR (50 MHz, CD₃OD): δ 199.14, 174.29, 162.39, 138.14, 130.29, 129.45, 127.88, 54.54, 39.65, 38.04, 37.74, 33.09, 30.78, 30.68, 30.58, 30.50, 30.13, 24.29, 23.75, 14.46; MS (ESI) *m/z* (%): 418.2 (100) (M+H)⁺. Anal. Calcd for C₂₅H₃₉NO₄: C, 71.91; H, 9.41; N, 3.35. Found: C, 71.81; H, 9.53; N, 3.22.

4.3. In vitro sPLA₂ assay

A continuous fluorimetric assay described previously was used to determine the inhibitory activity of compounds **GK111**, **GK112**, **GK122**, **GK126**, **GK141**, **GK144**, **GK145**, and **AX115**.²⁹

4.3.1. IC₅₀ value determination

IC₅₀ values for compounds **GK111**, **GK112**, **GK122**, **GK126** and **GK145** are reported as the mean of duplicate or triplicate analysis with standard deviations. All other compounds were screened at single doses and reported as >1.66 μM, or a % inhibition at 16.6 μM is given. IC₅₀ values were determined by nonlinear regression analysis of a semi-log plot of percent inhibition versus log of inhibitor concentration. Curves were fit to a variable slope sigmoidal dose–response curve using the Kaleidagraph software. Five inhibitor concentrations ranging from 10% to 90% inhibition were used for each IC₅₀ value determination.

4.3.2. Assay procedure

To seven wells of a 96-well microtiter plate was added 100 μL of solution A (27 μM bovine serum albumin, 50 mM KCl, 1 mM CaCl₂, 50 mM Tris–HCl, pH 8.0) followed by the desired concentration of inhibitor (1 μL in DMSO from serial-diluted stock solutions) or 1 μL of DMSO for control reactions. To the first well was added an additional 100 μL of solution A as a negative control. Solution B was prepared by mixing the appropriate amount of sPLA₂, depending on the specific activity, to Solution A. This solution was prepared immediately prior to each set of assays, to avoid loss of enzymatic activity due to sticking to the walls of the container. Solution B was delivered in 100 μL portions to all seven wells except the first well. Quickly after the addition of Solution B, the assay was initiated by the addition of 100 μL of Solution C (4.2 μM 1-hexadecanoyl-2-(1-pyrenedecanoyl)-sn-glycero-3-phosphoglycerol (pyrPG, Molecular Probes) vesicles in assay buffer (50 mM KCl, 1 mM CaCl₂, 50 mM Tris–HCl, pH 8.0)) to all seven wells. The fluorescence (excitation = 342 nm, emission = 395 nm) was read with a microtiter plate spectrophotometer (Fluorocount, Packard Instruments). Control reactions without enzyme or inhibitor were run with each assay of seven wells and the percent inhibition calculated from the initial slopes of fluorescence versus time. The amount of enzyme used per well are as follows: hGIIA, 6 ng; hGV, 12.5 ng; hGX, 17.7 ng; mGIIA, 3.4 ng; mGV, 12.7 ng; mGX, 10.7 ng. All of the recombinant mouse and human sPLA₂s were prepared as previously described.³⁸

4.4. Computational methods

4.4.1. Preparation of the GIIA sPLA₂ crystal structure

The crystal structures of the GIIA sPLA₂ enzyme which were deposited in the RCSB protein data bank with PDB IDs: 1DB4 holo form 2.20 Å X-ray resolution,¹⁰ 1DB5 holo form 2.80 Å X-ray resolution,¹⁰ 1J1A holo form 2.20 Å X-ray resolution,¹¹ 1KVO holo form 2.00 Å X-ray resolution¹² were downloaded. The objective was to judge which crystal structure is appropriate for the docking calculations. This was determined by using the following procedure: (i) using 'Superposition panel' of MAESTRO 9.0⁴² all the crystal structures were superimposed based on all the backbone atoms including beta carbons. The crystal structure with PDB ID: 1DB4 was chosen as a reference structure for the superposition (RMSD between: 1DB4–1DB5: 0.147 Å, 1DB4–1J1A: 0.746 Å, 1DB4–1KVO: 0.487 Å). No significant structural differences were observed as indicated by the RMSD values (Fig. 1 in Supplementary data); (ii) the active site region was examined to determine if the superimposed ligands can fit into the reference site without steric clashes. No significant steric clashes were observed; (iii) the active site region of all the crystal structures, in turn, was examined in order to determine

whether any residues in the superimposed protein differ appreciably in position or conformation from those in the reference site. No significant differences were observed. Even though all crystal structures are suitable, the 1DB4 PDB file was chosen for the molecular docking calculations because this file contains a single unit of the GIIA sPLA₂ enzyme co-crystallized with an indole inhibitor. The 1DB4 crystal structure was prepared using the 'Protein Preparation Wizard' panel⁴³ of Schrödinger Suite 2009. Using the 'Preprocess and analyze structure' tool, the bond orders were assigned, all the hydrogen atoms were added, the calcium ion was treated in order to have the correct geometry and the correct formal charge (+2), the disulfide bonds were assigned, and all the water molecules at a distance greater than 5 Å from any het group were deleted. Using EPIK 2.0,^{44,45} a prediction of het groups ionization and tautomeric states was performed. An optimization of the hydrogen bonding network was performed using the 'H-bond assignment' tool. Finally, using the 'Impref utility' the positions of the hydrogen atoms were optimized by keeping all the heavy atoms in place. The prepared structure was saved in PDB file format and was used as the input file in the docking calculations.

4.4.2. Preparation of the ligands

The crystallographic ligands and the 2-oxoamide ligands were sketched using the SYBYL 8.0 molecular sketcher.³⁶ All the hydrogen atoms were added to define the correct ionization and tautomeric states, and the oxygen atoms of the carboxylate and phosphonate groups were considered as equivalent with atom type for the oxygen atoms of O.co2. The molecules were subjected to energy minimization using the standard Tripos⁴⁶ molecular mechanics force field of the SYBYL 8.0 molecular modeling package, and the Powell⁴⁷ energy minimization algorithm with a gradient of 0.01 kcal mol⁻¹ Å⁻¹ was used for the minimization procedure.

4.4.3. Simulated annealing method

The investigation of the conformational space of each inhibitor, using the method of simulated annealing⁴⁸ was performed. Each inhibitor was heated at temperature 2000 K for 2000 fs and was cooled at a temperature 0 K for 10000 fs for 100 cycles. For the simulation, the Tripos⁴⁶ standard molecular mechanic force field was used. The dielectric function was selected to be distance dependent with a value of 1 for the distance-dependent dielectric constant and nonbonded cutoffs of 8.0 Å. The annealed structures were minimized using the Powell energy minimization algorithm with a gradient of 0.01 kcal mol⁻¹ Å⁻¹. For the simulated annealing the SYBYL 8.0³⁶ was used.

4.4.4. Molecular docking procedure

For the molecular docking calculation the genetic algorithm GOLD 4.1³¹ was used along with the standard GOLD scoring function GOLDScore.⁴⁹ The active site of the GIIA sPLA₂ was set as 6.0 Å around the native ligand. All the critical amino acids (Leu2, Val3, Phe5, His6, Ile9, Ala17, Ala18, Tyr21, His27, Gly29, Gly31, Asp48, Tyr51, Lys62 and Phe98) including the calcium ion and the His47/Asp91 catalytic dyad were considered in the active site. For the five water molecules, near the active site, the state 'Toggle' was specified, and the orientation of the hydrogen atoms of each water molecule was automatically optimized using the 'Spin' option. The geometry of the calcium ion was simulated by GOLD as octahedral with RMSD of 0.465 Å. For highest accuracy of the docking calculations, long search settings were used for the GOLD GA: 100 dockings with 100,000 GA operations per docking; the algorithm was not allowed to terminate early when the same solution was produced repeatedly. The GOLD algorithm supports flexible docking for the ligand, which is not depended on its initial conformation, and provides partial flexibility for the receptor.

Acknowledgments

The project is co-funded by the European Social Fund and National Resources (EPEAEK II) (G.K.) and by a grant from the National Institutes of Health (HL36235) (M.H.G.). V. D. Mouchlis was funded by the Research Promotion Foundation (RPF) (bilateral agreement CY-SLO/0407/06).

Supplementary data

Supplementary data associated with this article can be found, in the online version, at doi:10.1016/j.bmc.2010.12.030.

References and notes

- Burke, J. E.; Dennis, E. A. *Cardiovasc. Drugs Ther.* **2009**, *23*, 49.
- Leslie, C. C. *Prostaglandins Leukot. Essent. Fatty Acids* **2004**, *70*, 373.
- Bonventre, J. V.; Huang, Z.; Taheri, M. R.; O'Leary, E.; Li, E.; Moskowitz, M. A.; Sapirstein, A. *Nature* **1997**, *390*, 622.
- Uozumi, N.; Kume, K.; Nagase, T.; Nakatani, N.; Ishii, S.; Tashiro, F.; Komagata, Y.; Maki, K.; Ikuta, K.; Ouchi, Y.; Miyazaki, J.; Shimizu, T. *Nature* **1997**, *390*, 618.
- Lambeau, G.; Gelb, M. H. *Annu. Rev. Biochem.* **2008**, *77*, 495.
- Kramer, R. M.; Hession, C.; Johansen, B.; Hayes, G.; McGray, P.; Chow, E. P.; Tizard, R.; Pepinsky, R. B. *J. Biol. Chem.* **1989**, *264*, 5768.
- Scott, D. L.; White, S. P.; Browning, J. L.; Rosa, J. J.; Gelb, M. H.; Sigler, P. B. *Science* **1991**, *254*, 1007.
- Wery, J. P.; Schevitz, R. W.; Clawson, D. K.; Bobbitt, J. L.; Dow, E. R.; Gamboa, G.; Goodson, T., Jr.; Hermann, R. B.; Kramer, R. M.; McClure, D. B.; Mihelich, E. D.; Putnam, J. E.; Sharp, J. D.; Stark, D. H.; Teater, C.; Warrick, M. W.; Jones, N. D. *Nature* **1991**, *352*, 79.
- Magrioti, V.; Kokotos, G. *Expert Opin. Ther. Patents* **2010**, *20*, 1.
- Schevitz, R. W.; Bach, N. J.; Carlson, D. G.; Chirgadze, N. Y.; Clawson, D. K.; Dillard, R. D.; Draheim, S. E.; Hartley, L. W.; Jones, N. D.; Mihelich, E. D.; Olkowski, J. L.; Snyder, D. W.; Sommers, C.; Wery, J.-P. *Nat. Struct. Biol.* **1995**, *2*, 458.
- Hansford, K. A.; Reid, R. C.; Clark, C. I.; Tyndall, J. D.; Whitehouse, M. W.; Guthrie, T.; McGeary, R. P.; Schafer, K.; Martin, J. L.; Fairlie, D. P. *ChemBioChem* **2003**, *4*, 181.
- Cha, S. S.; Lee, D.; Adams, J.; Kurdyla, J. T.; Jones, C. S.; Marshall, L. A.; Bolognese, B.; Abdel-Meguid, S. S.; Oh, B. H. *J. Med. Chem.* **1996**, *39*, 3878.
- Mouchlis, V. D.; Mavromoustakos, T. M.; Kokotos, G. *J. Comput. Aided Mol. Des.* **2010**, *24*, 107.
- Tomoo, K.; Yamane, A.; Ishida, T.; Fujii, S.; Ikeda, K.; Iwama, S.; Katsumura, S.; Sumiya, S.; Miyagawa, H.; Kitamura, K. *Biochim. Biophys. Acta* **1997**, *1340*, 178.
- Mouchlis, V. D.; Mavromoustakos, T. M.; Kokotos, G. *J. Chem. Inf. Model.* **2010**, *50*, 1589.
- Pintore, M.; Mombelli, E.; Wechman, C.; Chretien, J. R. *Anti-Inflammatory Anti-Allergy Agents Med. Chem.* **2006**, *5*, 175.
- Taylor, R. D.; Jewsbury, P. J.; Essex, J. W. *J. Comput. Aided Mol. Des.* **2002**, *16*, 151.
- Halperin, I.; Ma, B.; Wolfson, H.; Nussinov, R. *Proteins* **2002**, *47*, 409.
- Wei, D.; Jiang, X.; Zhou, L.; Chen, J.; Chen, Z.; He, C.; Yang, K.; Liu, Y.; Pei, J.; Lai, L. *J. Med. Chem.* **2008**, *51*, 7882.
- Kokotos, G.; Kotsovolou, S.; Six, D. A.; Constantinou-Kokotou, V.; Beltzner, C. C.; Dennis, E. A. *J. Med. Chem.* **2002**, *45*, 2891.
- Kokotos, G.; Six, D. A.; Loukas, V.; Smith, T.; Constantinou-Kokotou, V.; Hadjipavlou-Litina, D.; Kotsovolou, S.; Chiou, A.; Beltzner, C. C.; Dennis, E. A. *J. Med. Chem.* **2004**, *47*, 3615.
- Constantinou-Kokotou, V.; Peristeraki, A.; Kokotos, C. G.; Six, D. A.; Dennis, E. A. *J. Pept. Sci.* **2005**, *11*, 431.
- Yaksh, T. L.; Kokotos, G.; Svensson, C. I.; Stephens, D.; Kokotos, C. G.; Fitzsimmons, B.; Hadjipavlou-Litina, D.; Hua, X. Y.; Dennis, E. A. *J. Pharmacol. Exp. Ther.* **2006**, *316*, 466.
- Stephens, D.; Barbayianni, E.; Constantinou-Kokotou, V.; Peristeraki, A.; Six, D. A.; Cooper, J.; Harkewicz, R.; Deems, R. A.; Dennis, E. A.; Kokotos, G. *J. Med. Chem.* **2006**, *49*, 2821.
- Six, D. A.; Barbayianni, E.; Loukas, V.; Constantinou-Kokotou, V.; Hadjipavlou-Litina, D.; Stephens, D.; Wong, A. C.; Magrioti, V.; Moutevelis-Minakakis, P.; Baker, S. F.; Dennis, E. A.; Kokotos, G. *J. Med. Chem.* **2007**, *50*, 4222.
- Antonopoulou, G.; Barbayianni, E.; Magrioti, V.; Cotton, N.; Stephens, D.; Constantinou-Kokotou, V.; Dennis, E. A.; Kokotos, G. *Bioorg. Med. Chem.* **2008**, *16*, 10257.
- Barbayianni, E.; Stephens, D.; Grkovich, A.; Magrioti, V.; Hsu, Y. H.; Dolatzas, P.; Kalogiannidis, D.; Dennis, E. A.; Kokotos, G. *Bioorg. Med. Chem.* **2009**, *17*, 4833.
- Dess, D. B.; Martin, J. C. *J. Am. Chem. Soc.* **1991**, *113*, 7277.
- Smart, B. P.; Pan, Y. H.; Weeks, A. K.; Bollinger, J. G.; Bahnson, B. J.; Gelb, M. H. *Bioorg. Med. Chem.* **2004**, *12*, 1737.
- Burke, J. E.; Babakhani, A.; Gorfe, A. A.; Kokotos, G.; Li, S.; Woods, V. L., Jr.; McCammon, J. A.; Dennis, E. A. *J. Am. Chem. Soc.* **2009**, *131*, 8083.
- GOLD 4.1, CCDC, Cambridge, UK, 2009.
- Verdonk, M. L.; Chessari, G.; Cole, J. C.; Hartshorn, M. J.; Murray, C. W.; Nissink, J. W.; Taylor, R. D.; Taylor, R. *J. Med. Chem.* **2005**, *48*, 6504.
- Verdonk, M. L.; Cole, J. C.; Hartshorn, M. J.; Murray, C. W.; Taylor, R. D. *Proteins* **2003**, *52*, 609.
- Scott, D. L.; Sigler, P. B. *Adv. Protein Chem.* **1994**, *45*, 53.
- Li, B.; Liu, Z.; Zhang, L. *J. Chem. Inf. Model.* **2009**, *49*, 1725.
- SYBYL, molecular modeling software packages, version 8.0; Tripos Inc.: 1699 South Hanley Rd., St. Louis, MO 63144-2917, 2007.
- Reid, R. C. *Curr. Med. Chem.* **2005**, *12*, 3011.
- Singer, A. G.; Ghomashchi, F.; Le Calvez, C.; Bollinger, J.; Bezzine, S.; Rouault, M.; Sadilek, M.; Nguyen, E.; Lazdunski, M.; Lambeau, G.; Gelb, M. H. *J. Biol. Chem.* **2002**, *277*, 48535.
- Oslund, R. C.; Cermak, N.; Gelb, M. H. *J. Med. Chem.* **2008**, *51*, 4708.
- Rosenson, R. S. *Cardiovasc. Drugs Ther.* **2009**, *23*, 93.
- Garcia-Garcia, H. M.; Serruys, P. W. *Curr. Opin. Lipidol.* **2009**, *20*, 327.
- MAESTRO, version 9.0; Schrödinger, LLC: New York, NY, 2009.
- Schrödinger Suite 2009 Protein Preparation Wizard; EPIK version 2.0; Schrödinger, LLC: New York, NY, 2009; Impact version 5.5; Schrödinger, LLC: New York, NY, 2009; Prime version 2.1; Schrödinger, LLC: New York, NY, 2009.
- EPIK, version 2.0; Schrödinger, LLC: New York, NY, 2009.
- Shelley, J. C.; Cholleti, A.; Frye, L. L.; Greenwood, J. R.; Timlin, M. R.; Uchimaya, M. *J. Comput. Aided Mol. Des.* **2007**, *21*, 681.
- Clark, M.; Crammer, D. R., III; Van Opdenbosch, N. *J. Comput. Chem.* **1989**, *10*, 982.
- Powell, D. J. *Math. Program.* **1977**, *12*, 241.
- Kirkpatrick, S.; Gelatt, C. D., Jr.; Vecchi, M. *Science* **1983**, *220*, 671.
- Jones, G.; Willett, P.; Glen, R. C.; Leach, A. R.; Taylor, R. *J. Mol. Biol.* **1997**, *267*, 727.